On the Predictability of Quasi-Geostrophic Flow: The Effects of Beta and Baroclinicity

GEOFFREY K. VALLIS

Scripps Institution of Oceanography, La Jolla, CA 92093

(Manuscript received 24 May 1982, in final form 18 August 1982)

ABSTRACT

The equilibrium statistics and predictability properties of one- and two-layer quasi-geostrophic flow are examined with the aid of a numerical model. The effect of beta in one-layer flow is to slow the transfer of energy into larger scales and to increase the predictability. In two-layer flow, when beta is zero, energy enters the system via baroclinic instability of the mean flow at very large scales and most energy transfer is confined to low wavenumbers. When beta is non-zero, energy enters at higher wavenumbers (in baroclinic modes mainly) before cascading preferentially to lower wavenumber zonal barotropic modes. The predictability of two-layer flow is not significantly altered by beta, because beta increases the range of wavenumber over which significant nonlinear energy transfer occurs. The predictability times of the long waves are found to be always larger than those of the short waves, even when the initial error is spread evenly across wavenumbers. Reducing the mean baroclinicity increases the predictability time. Two-layer flow is less predictable than one-layer flow of the same barotropic energy, because of the effects of baroclinic instability and the transfer of energy from baroclinic modes.

1. Introduction

Predictability theory occupies a central role in much meteorological research, and naturally so, considering its fundamental nature and the socio-economic importance of weather and climate forecasts. Our ability to forecast the weather depends on two factors. One is the extent to which those models used in weather forecasting are able to mimic the real atmosphere. For example, inadequate resolution and imperfect physical parameterizations will give rise to inaccurate forecasts. Given a perfect model, however, perfect forecasts would not necessarily ensue: unavoidable errors in the initial conditions, concentrated mainly in the smaller scales of motion, amplify and cascade into the larger scales, resulting in a prediction with no skill. This is referred to as the inherent unpredictability of the atmosphere, and was probably first addressed by Thompson (1957). It is this aspect which will be discussed in this paper.

Early work in the 1960's with general circulation models (GCM's) (e.g., Charney *et al.*, 1966) suggested error doubling times of about 3 days, the error doubling time being largest initially, decreasing for smaller wavenumber and larger error fields. Another approach was taken by Lorenz (1969), Leith (1971) and Leith and Kraichnan (1972), in the use of closure theories of turbulence applied to two-dimensional flow. Such studies achieved high resolution, and hence high Reynolds numbers, and yielded predictability times of ~1–3 weeks, in qualitative agreement with GCM's.

In an attempt to bridge the somewhat alarming gap between the methods (if not the results) of these two types of studies, Lilly (1972) performed a direct, grid-point, numerical integration of a simplified hydrodynamical set of equations—the barotropic f-plane vorticity, or the two-dimensional turbulence equations. This work has been extended by Basdevant *et al.* (1981) and Holloway (1982) to include the effects of differential rotation, the beta effect, and finite equivalent depths. The aim of this type of research is not to ascertain quantitatively the limits to predictability in the earth's atmosphere, but to examine the influence of a variety of mechanisms, such as nonlinear transfer and wave propagation, on the gradual loss of information as a forecast proceeds.

The study presented herein extends this work to include the effects of baroclinicity; in particular I am concerned with the combined effects of planetary wave propagation and baroclinic instability. For example, does the Rhines effect, the slowing down of nonlinear energy transfer because of wave propagation, affect a two-layer model in the same way as a one-layer model? Does a baroclinic model have similar predictability properties to a barotropic model? Also, does the form and magnitude of the initial error affect its subsequent growth? The tool used is possibly the simplest model containing these mechanisms, a two-layer quasi-geostrophic beta plane model. The discussion in this paper will be couched in meteorological terms and dimensional variables, but it is hoped the paper will also be of interest to oceanographers and turbulence theoreticians. Section 2 de-

scribes the model used in this study. In Section 3 the equilibrium fields and spectra are discussed. Section 4 examines the predictability properties of the barotropic simulations. The two-layer simulations are described in Section 5. Section 6 summarizes and concludes.

2. Model

The potential vorticity equation in a multi-level model at an interior level n is

$$\frac{\partial}{\partial t} q_n + J(\psi_n, q_n) + \beta \frac{\partial \psi_n}{\partial x} = +D_n, \tag{1}$$

where

$$q_n = \nabla^2 \psi_n + \tfrac{1}{2}\lambda^2(\psi_{n+2} + \psi_{n-2} - 2\psi_n),$$
$$\lambda^2 = 2f_0^2/\sigma\Delta p^2,$$

and D_n is the dissipation term and $\beta = \partial f/\partial y$, where f is the Coriolis parameter. For a two-level model with zero pressure vertical velocity at the boundaries, we have in standard notation

$$\left.\begin{aligned} \frac{\partial}{\partial t} q_1 + J(\psi_1, q_1) + \beta \frac{\partial \psi_1}{\partial x} &= +D_1 \\ \frac{\partial}{\partial t} q_3 + J(\psi_3, q_3) + \beta \frac{\partial \psi_3}{\partial x} &= +D_3 \end{aligned}\right\}, \tag{2}$$

where

$$\left.\begin{aligned} q_1 &= \nabla^2 \psi_1 + \frac{\lambda^2}{2}(\psi_3 - \psi_1) \\ q_3 &= \nabla^2 \psi_3 + \frac{\lambda^2}{2}(\psi_1 - \psi_3) \end{aligned}\right\}. \tag{3}$$

Assume that the total streamfunction may be expressed as that resulting from a constant mean shear across the domain, plus an eddy component $\hat{\psi}$. Then

$$\left.\begin{aligned} \psi_1 &= -U_1 y + \hat{\psi}_1 \\ \psi_3 &= -U_3 y + \hat{\psi}_3 \end{aligned}\right\}. \tag{4}$$

Substituting (4) into (2) yields

$$\frac{\partial}{\partial t}\hat{q}_1 + J(\hat{\psi}_1, \hat{q}_1) + \beta \frac{\partial \hat{\psi}_1}{\partial x} = -\frac{\lambda^2}{2}\left(U_1 \frac{\partial \hat{\psi}_3}{\partial x} - U_3 \frac{\partial \hat{\psi}_1}{\partial x}\right) - U_1 \frac{\partial}{\partial x}\nabla^2 \hat{\psi}_1 + D_1, \tag{5}$$

$$\frac{\partial}{\partial t}\hat{q}_3 + J(\hat{\psi}_3, \hat{q}_3) + \beta \frac{\partial \hat{\psi}_3}{\partial x} = \frac{\lambda^2}{2}\left(U_1 \frac{\partial \hat{\psi}_3}{\partial x} - U_3 \frac{\partial \hat{\psi}_1}{\partial x}\right) - U_3 \frac{\partial}{\partial x}\nabla^2 \hat{\psi}_3 + D_3, \tag{6}$$

where $\hat{q}_1 = \nabla^2 \hat{\psi}_1 + \tfrac{1}{2}\lambda^2(\hat{\psi}_3 - \hat{\psi}_1)$ and similarly for $\hat{q}_3$. The carets will subsequently be dropped. The use of a constant mean shear is clearly artificial, but it is a convenient way of specifying the mean baroclinicity. On a beta-plane, the twin requirements of a mean temperature gradient across the domain and boundary conditions such as periodicity or no-slip or free-slip walls along the northern and southern edges, are difficult to satisfy simultaneously because of the dual use of the streamfunction in specifying the mean temperature

$$T = \frac{2f_0}{R}(\psi_1 - \psi_3),$$

and the velocity

$$u = -\frac{\partial \psi}{\partial y}, \quad v = \frac{\partial \psi}{\partial x}.$$

It is possible to do so by using a different basis set (in a spectral formulation) for the zonally averaged and eddy components (e.g., Lorenz, 1963), although this leads to aliasing if a pure transform method is used and seems unnecessarily complicated for our needs. Salmon (1980) derives an *ad hoc* formula giving the rate of change of the mean shear, based on energetic considerations although he found the variations about its mean value were less than 10% of its average, normally highly supercritical, value. The mean shear will be set to a constant value here, for a given integration.

Dissipation is parameterized as follows:

$$D_1 = \nu\nabla^6 \psi_1,$$
$$D_3 = \nu\nabla^6 \psi_3 + \alpha\nabla^2 \psi_3.$$

The $\alpha\nabla^2\psi$ term represents the effects of surface drag. It may alternatively be included by supposing the upward velocity at the lower boundary is not zero, but is given by Ekman theory; the term then appears in the lower boundary condition on the streamfunction, but with a formally, and physically, identical effect. The value of α used is (1/3) days^{-1}. The term $\nu\nabla^6\psi$ is necessary to prevent the build-up of enstrophy in high wavenumbers. The value of ν is empirically determined to be such that the energy spectra appeared smooth near the cutoff wavenumber. Its value is 8.75 10^{14} m^4 s^{-1}. It is found that the total energy dissipation by the high-order friction is a few percent of the total dissipation. It is only larger than the surface drag above wavenumber 28 (20 in the single-layer experiments).

Eqs. (5) and (6) are integrated using a spectral code with periodic boundary conditions in both directions. The Jacobian terms are evaluated using Orszag's (1971) alias-free staggered-grid algorithm, ensuring exact conservation of energy and enstrophy. Truncation occurs at approximately wavenumber 32. The domain is square and of physical size (2.25×10^7 m)^2. Time integration is by leapfrog, with a Robert-

Asselin filter (Asselin, 1972) with filter parameter 0.02. A timestep of 0.75 h is generally used.

Some barotropic integrations will also be described. The governing equation now is

$$\frac{\partial}{\partial t}\nabla^2\psi + J(\psi, \nabla^2\psi) + \beta\frac{\partial\psi}{\partial x} = F + D, \qquad (7)$$

where D is the dissipation term $\alpha\nabla^2\psi + \nu\nabla^6\psi$; ν has the same value as in the two-level experiments, and α is reduced to (1/12) days^{-1}. Since baroclinic instability no longer occurs, its effects are crudely simulated using a Markovian random forcing formulation (e.g., Williams, 1978). Thus, at time-step n

$$F_n = R_nF_{n-1} + (1 - R_n^2)^{1/2}G_nA, \qquad (8)$$

where $R_n = 0.98$ for a timestep of 0.75 h.

G_n is a number with unit amplitude and a random phase, different for each wavenumber, and A is the forcing amplitude. A is zero except in the wavenumber band $k = 6, 7, 8$, wherein its value increases linearly with k_x (the x wavenumber) with an average value of 10^{12} s^{-2}. The forcing differs from baroclinic instability in that G is uncorrelated with the flow.

3. Equilibrium fields and energy budgets

a. Energy transfer: Some simple considerations

Before presenting numerical solutions to (5) and (6), it will be shown that the general characteristics of energy transfer in two-layer flow can be inferred from relatively simple analytic arguments based on the quadratic constants of the motion and weakly nonlinear theory. These will be of help in interpreting the numerical solutions. It is convenient to first write (5) and (6) in terms of the baroclinic (τ) and barotropic (ψ) streamfunctions defined by

$$\psi = (\psi_1 + \psi_3)/2,$$
$$\tau = (\psi_1 - \psi_3)/2.$$

Adding and subtracting (5) and (6) gives

$$\frac{\partial}{\partial t}\nabla^2\psi + J(\psi, \nabla^2\psi) + J(\tau, \nabla^2\tau) + \beta\frac{\partial\psi}{\partial x} = {}_\psi F + {}_\psi D, \qquad (9)$$

$$\frac{\partial}{\partial t}(\nabla^2 - \lambda^2)\tau + J[\psi, (\nabla^2 - \lambda^2)\tau] + J(\tau, \nabla^2\psi) + \beta\frac{\partial\tau}{\partial x} = {}_\tau F + {}_\tau D, \qquad (10)$$

where

$${}_\psi D = \{\nu\nabla^6\psi + (\alpha\nabla^2\psi_3)/2\},$$
$${}_\tau D = \{\nu\nabla^6\tau - (\alpha\nabla^2\psi_3)/2\},$$

$${}_\psi F = -\left\{U_1\frac{\partial\nabla^2}{\partial x}\psi_1 + U_3\frac{\partial}{\partial x}\nabla^2\psi_3\right\}\Big/2,$$

$${}_\tau F = -\frac{\lambda^2}{2}\left\{U_1\frac{\partial\psi_3}{\partial x} - U_3\frac{\partial\psi_1}{\partial x}\right\},$$
$$-\frac{U_1}{2}\frac{\partial}{\partial x}\nabla^2\psi_1 + \frac{U_3}{2}\frac{\partial}{\partial x}\nabla^2\psi_3.$$

Without loss of generality, we may set $U_1 = -U_3 = U$ giving

$${}_\psi F = -U\frac{\partial}{\partial x}\nabla^2\tau,$$

$${}_\tau F = -\frac{U\partial}{\partial x}(\lambda^2 + \nabla^2)\psi.$$

This shows that ${}_\tau F$ vanishes for $k = \lambda$. The spectral barotropic and baroclinic energy budgets are obtained by first writing (9) and (10) in spectral form, and multiplying each component by $\psi_{\mathbf{k}}^*$ or $\tau_{\mathbf{k}}^*$, respectively, where the asterisk refers to the complex conjugate.

This yields

$$\frac{d}{dt}k^2|\psi_{\mathbf{k}}|^2 = \mathrm{Re}\{{}_\psi F_{\mathbf{k}}\psi_{\mathbf{k}}^* + {}_\psi D_{\mathbf{k}}\psi_{\mathbf{k}}^* + {}_\psi J_{\mathbf{k}}\psi_{\mathbf{k}}^*\}, \qquad (11)$$

$$\frac{d}{dt}\{(k^2 + \lambda^2)|\tau_{\mathbf{k}}|^2\} = \mathrm{Re}\{{}_\tau F_{\mathbf{k}}\tau_{\mathbf{k}}^* + {}_\tau D_{\mathbf{k}}\tau_{\mathbf{k}}^* + {}_\tau J_{\mathbf{k}}\tau_{\mathbf{k}}^*\}, \qquad (12)$$

where ${}_\psi J_{\mathbf{k}}$ and ${}_\tau J_{\mathbf{k}}$ are the spectral components of all of the Jacobians appearing in (9) and (10), respectively, and where

$$\left.\begin{aligned}[\psi(x, y, t), \tau(x, y, t)] &= \sum_{\mathbf{k}}[\psi_{\mathbf{k}}(t), \tau_{\mathbf{k}}(t)]\exp(i\mathbf{k}\cdot\mathbf{x}) \\ (\psi_{\mathbf{k}}, \tau_{\mathbf{k}}) &= (\psi_{-\mathbf{k}}^*, \tau_{-\mathbf{k}}^*)\end{aligned}\right\}. \qquad (13)$$

The terms involving beta vanish identically from (11) and (12). The energy equations for each spectral component are real because of the condition (13), which also ensures the reality of the streamfunction. Summing over all spectral components, and adding the baroclinic and barotropic modes, gives the integral constraint for unforced, inviscid flow:

$$\frac{d}{dt}\sum_{\mathbf{k}}(k^2|\psi_{\mathbf{k}}|^2 + (k^2 + \lambda^2)|\tau_{\mathbf{k}}|^2) = 0. \qquad (14)$$

The enstrophy budget is obtained by multiplying the spectral forms of (9) and (10) by $(q_1 + q_2)/2$ and $(q_1 - q_2)/2$, respectively. For unforced, inviscid flow the integral constraint on the enstrophy is found to be

$$\frac{d}{dt}\sum_{\mathbf{k}}\{k^4|\psi_{\mathbf{k}}|^2 + (k^2+\lambda^2)^2|\tau_{\mathbf{k}}|^2\} = 0. \quad (15)$$

If, and only if, beta is zero then the enstrophy for each layer [or equivalently the barotropic enstrophy $\sum_{\mathbf{k}} k^4|\psi_{\mathbf{k}}|^2$ and the baroclinic enstrophy $\sum_{\mathbf{k}} (k^2+\lambda^2)^2 \times |\tau_{\mathbf{k}}|^2$] is separately conserved.

The advantages of writing the budgets in terms of the baroclinic and barotropic modes lie in the simplicity of the triad interactions and the form of the integral constraints. For we see immediately from (14) and (15) that a baroclinic mode is formally similar to a barotropic mode, provided we make the replacement in wavenumber, i.e.,

$$k^2 \rightarrow k^2 + \lambda^2.$$

Salmon (1980) has shown how a knowledge of the integral constraints can be used to deduce the general isotropic movement of energy in a two-layer model, in a similar fashion to their use in two-dimensional turbulence (e.g., Fjørtoft, 1953). Thus, in a purely barotropic triad, energy is transferred predominantly to lower wavenumbers. In a mixed triad (ψ, τ, τ), energy will go predominantly to lower total wavenumber k' defined by $k'^2 = k^2 + \lambda^2$ in a baroclinic mode, and $k'^2 = k^2$ in a barotropic mode. Transfer of baroclinic energy may be toward higher wavenumber, provided there is some energy conversion to a barotropic mode (which on the interval $1 \leqslant k^2 \leqslant \lambda^2$ will always have lower total wavenumber). In the oceanographic, and more general, case of two layers of different equivalent depths, two baroclinic modes may interact with a third baroclinic mode. This does not occur here, because the two layers are of equal depth.

b. *Weakly nonlinear theory*

Use of the quadratic invariants gives no information regarding the anisotropic energy spectra. Weakly nonlinear theory (e.g., Holloway, 1979) is useful in this respect, since it yields information about the frequencies of unstable modes. The unforced, inviscid versions of (9) and (10) are rewritten, after suitable nondimensionalization, as

$$\frac{\partial}{\partial t}\nabla^2\psi + \frac{\partial\psi}{\partial x} + \epsilon J(\psi, \nabla^2\psi) + \epsilon J(\tau, \nabla^2\tau) = 0, \quad (16)$$

$$\frac{\partial}{\partial t}(\nabla^2 - \lambda^2)\tau + \frac{\partial\tau}{\partial x} + \epsilon J(\psi, (\nabla^2 - \lambda^2)\tau) + \epsilon J(\tau, \nabla^2\psi) = 0, \quad (17)$$

where $\epsilon = k_0^2 U_s \beta^{-1}$ is a measure of wave-steepness

k_0 = 1/(length scale)

and

U_s = velocity scale (e.g., rms velocity).

Asymptotic theory suggests that the streamfunction be expanded in powers of ϵ (assumed small). Thus

$$\left.\begin{aligned}\psi &= {}_0\psi + \epsilon\,{}_1\psi + \epsilon^2\,{}_2\psi + \cdots\\ \tau &= {}_0\tau + \epsilon\,{}_1\tau + \epsilon^2\,{}_2\tau + \cdots\end{aligned}\right\}. \quad (18)$$

Substituting (18) into (16) and (17), and equating powers of ϵ gives, in spectral form

$$\left.\begin{aligned}L\,{}_0\psi_{\mathbf{k}} &= 0\\ L'\,{}_0\tau_{\mathbf{k}} &= 0\end{aligned}\right\}, \quad (19)$$

$$\left.\begin{aligned}L\,{}_1\psi_{\mathbf{k}} &= \sum\{A_{\mathbf{kpq}}\,{}_0\psi_{\mathbf{p}}\,{}_0\psi_{\mathbf{q}}\} + \sum\{A_{\mathbf{kpq}}\,{}_0\tau_{\mathbf{p}}\,{}_0\tau_{\mathbf{q}}\}\\ L'\,{}_1\tau_{\mathbf{k}} &= \sum A_{\mathbf{k'pq'}}\,{}_0\psi_{\mathbf{p}}\,{}_0\tau_{\mathbf{q}}\end{aligned}\right\}, \quad (20)$$

where the summations are over all $\mathbf{p}$ and $\mathbf{q}$ satisfying $\mathbf{p} + \mathbf{q} = \mathbf{k}$, and

$$L = \frac{d}{dt} + i\sigma,$$

$$L' = \frac{d}{dt} + i\sigma',$$

$$\sigma = \frac{k_x}{k_x^2 + k_y^2}, \quad \sigma' = \frac{k_x}{k_x^2 + k_y^2 + \lambda^2},$$

$$A_{\mathbf{kpq}} = (p^2 - q^2)(p_x q_y - p_y q_x)/(k^2),$$

$$A_{\mathbf{k'pq'}} = [p^2 - (q^2 + \lambda^2)](p_x q_y - p_y q_x)/(k^2 + \lambda^2).$$

Resonant interactions are the only interactions which significantly transfer energy between modes in the presence of beta. These occur when the combined frequency of two zeroth-order waves (Rossby waves) is the same as the natural frequency of a first-order mode. Secular terms then arise in the solutions of (20) (Kenyon, 1964). These would invalidate the solution after a finite time, and are avoided by a multiple time scale expansion (see Bender and Orszag, 1978, Chap. xi) in which one writes

$${}_0\psi = \bar{\psi}(t_1)e^{i\sigma t},$$

and similarly for ${}_0\tau$, where $t_1 = \epsilon t$ is a "slow" timescale. Secular terms are avoided by choosing the envelope ($\bar{\psi}$ and $\bar{\tau}$) solutions to satisfy, for a particular resonant triad,

$$\frac{d}{dt_1}\,{}_0\bar{\psi}_{\mathbf{k}} = A_{\mathbf{kpq}}\,{}_0\bar{\psi}_{\mathbf{p}}\,{}_0\bar{\psi}_{\mathbf{q}}, \quad (21)$$

and cyclically, this being the purely barotropic interaction, and for the mixed mode interactions

$$\left.\begin{aligned}\frac{d}{dt_1}\,{}_0\bar{\psi}_{\mathbf{k}} &= A_{\mathbf{kpq}}\,{}_0\bar{\tau}_{\mathbf{p}}\,{}_0\bar{\tau}_{\mathbf{q}}\\ \frac{d}{dt_1}\,{}_0\bar{\tau}_{\mathbf{p}} &= A_{\mathbf{p'q'k}}\,{}_0\bar{\tau}_{\mathbf{q}}\,{}_0\bar{\psi}_{\mathbf{k}}\\ \frac{d}{dt_1}\,{}_0\bar{\tau}_{\mathbf{q}} &= A_{\mathbf{q'kp'}}\,{}_0\bar{\tau}_{\mathbf{p}}\,{}_0\bar{\psi}_{\mathbf{k}}\end{aligned}\right\}. \tag{22}$$

The problem of solving (21) or (22) is only tractable if attention is restricted to one triad. To consider interactions among all modes requires a numerical approach.

The linear stability properties of a barotropic triad (21) are the same as those in purely two-dimensional turbulence. Thus the mode of intermediate scale, and largest frequency is unstable to disturbances of larger or smaller scale. The extension to two layers (i.e., the mixed-mode problem) is relatively straightforward. It can be shown (Jones, 1979) that the mode of intermediate *total* wavenumber (be it a barotropic or baroclinic mode) is unstable. Now the resonance condition for a triad with modes labelled 1, 2, 3 (i.e., with wavenumber $\mathbf{k}_i$ and natural frequency σ_i) is

$$\sigma_1 + \sigma_2 + \sigma_3 = 0, \tag{23}$$

where

$$\sigma_i = \frac{k_{ix}}{k'^2}, \tag{24}$$

and k'^2 is the *total* wavenumber squared (i.e., including the effects of the Rossby radius in baroclinic modes). The interaction condition is

$$\left.\begin{aligned}k_{1x} + k_{2x} + k_{3x} &= 0\\ k_{1y} + k_{2y} + k_{3y} &= 0\end{aligned}\right\}. \tag{25}$$

We can always order the frequencies such that $\sigma_1 = -(\sigma_2 + \sigma_3)$, where σ_2 and σ_3 are of the same sign. Thus, σ_1 is the highest frequency. Then, using (24) and (25)

$$\sigma_2(k_2'^2 - k_1'^2) = \sigma_3(k_1'^2 - k_3'^2);$$

therefore

$$k_2'^2 > k_1'^2 > k_3'^2$$

or

$$k_2'^2 < k_1'^2 < k_3'^2.$$

Hence the wave of largest frequency is the wave of intermediate "scale," if account is taken of the inverse deformation radius λ. Thus Hasselmann's (1967) criterion that the unstable member of a resonantly interacting triad is that with the largest frequency, is satisfied.

The transfer of energy in resonant triads is to first order completely unaffected by beta since (22) and (21) are identical with the triad equation when beta is zero. However, the set of resonant triads is small in comparison to the set of all interacting triads since the extra condition (23) must also be satisfied. Thus beta will slow down any energy cascade in which energy is injected at comparable scales. Note that beta will also slow down any transfer of baroclinic energy to smaller scales, as well as the transfer of barotropic energy to larger scales, an effect familiar from two-dimensional flow (Rhines, 1975).

Since the wave of highest frequency is also unstable in two-layer flow, wave propagation will cause the preferential transfer of energy to smaller frequencies. Since the simultaneous occurrence of small frequencies, demanded by weakly nonlinear theory, and large scales, demanded by the integral constraints, can only be satisfied by zonal or near zonal flow [see Eq. (24)], then in two-layer flow as well as barotropic flow, planetary wave propagation favors the production of zonal currents. Again, however, zonal currents cannot be produced by purely resonant interactions, since then the interaction coefficient vanishes. Furthermore, large-scale barotropic waves are stable to resonant perturbations of smaller scales, whether barotropic or baroclinic. Hence zonal barotropic currents with meridional scale at approximately the Rhines wavenumber $k_\beta \approx (\beta/2U)^{1/2}$ are the likely end state of two-layer flow (apart from the effects of baroclinic instability and friction). In the next section numerical simulations are used in order to examine the flow quantitatively, and to look at the complications caused by baroclinic instability.

c. *Numerical simulations*

Numerical simulations allow one to relax the assumption of vertical homogeneity, i.e., that τ and ψ are uncorrelated, often used in semi-analytic closure theories, if only for tractability (Salmon, 1978). Actually, vertical homogeneity is not a prohibitive assumption in comparisons with direct two-layer simulations, since only deep linear eddies are allowed in any case and since the general nature of the nonlinear interactions is unaltered. The advantage of numerical simulations over closure lies more in the complete absence of arbitrary phenomenological coefficients, provided sufficient resolution can be achieved.

This subsection describes the equilibrium, time-averaged fields resulting when (9) and (10) were stepped to equilibrium. Table 1 lists the parameters used. In a barotropic simulation, it is relatively easy to isolate the effects of beta on the flow, since all forcing and dissipation mechanisms may be held constant, but it is somewhat more difficult in two-layer flow since the stability properties are profoundly affected by beta. In the two-layer experiments B1 and NB, the inviscid supercriticality of the shear (i.e., its value above the level required for linear instability) was set equal. It then turned out that the equilibrium, time-averaged, total energy in B1 and NB was approximately the same. In B2, the shear was reduced.

TABLE 1. Experiment parameters and selection of results. Predictability time is the time taken for error energy to reach 90% of its final value.

Experiment	B1	B2	NB	1B	1NB
Number of levels	2	2	2	1	1
Value of beta	1.5×10^{-11}	1.5×10^{-11}	0	1.5×10^{-11}	0
Shear $(u_1 - u_3)$ [m s^{-1}]	7.5	4.0	3.66	—	—
Supercriticality (inviscid) [m s^{-1}]	3.66	0.16	3.66	—	—
λ (inverse deformation radius, expressed as a wavenumber)	10	10	10	—	—
Total energy [J m^{-2}]	7.0×10^5	1.2×10^5	7.0×10^5	4.2×10^5	4.2×10^5
Barotropic energy	3.7×10^5	5.4×10^4	2.8×10^5	4.2×10^5	4.2×10^5
U_{rms} [m s^{-1}]	8.6	3.3	7.5	9.2	9.2
k_β $(\beta/2U)^{1/2}$ (non-dimensionalized)	3.3	5.3	—	3.2	—
Eddy turnover time (days)	0.85	1.62	1.04	—	—
Error doubling time (days)	1.0	2.1	1.1	2.3	1.85
Predictability time (days)	11	19	12.5	25	20

All other parameters (aside from beta) were unchanged. In B1 and B2, beta is given the realistic value of 1.5×10^{-11} s^{-1}, whereas in NB it is set to zero.

The following energy and enstrophy spectra and transfers may be defined for the two-level model:

$$\begin{aligned} EC(\mathbf{k}) &= (k^2 + \lambda^2)|\tau_\mathbf{k}|^2, \\ ET(\mathbf{k}) &= k^2|\psi_\mathbf{k}|^2, \\ EN(\mathbf{k}) &= [k^4|\psi_\mathbf{k}|^2 + (k^2 + \lambda^2)^2|\tau_\mathbf{k}|^2], \\ DC(\mathbf{k}) &= \mathrm{Re}({}_\tau D_\mathbf{k} \tau_\mathbf{k}^*), \\ DT(\mathbf{k}) &= \mathrm{Re}({}_\psi D_\mathbf{k} \psi_\mathbf{k}^*), \\ FC(\mathbf{k}) &= \mathrm{Re}({}_\tau F_\mathbf{k} \tau_\mathbf{k}^*), \\ FT(\mathbf{k}) &= \mathrm{Re}({}_\psi F_\mathbf{k} \psi_\mathbf{k}^*), \\ TC(\mathbf{k}) &= \mathrm{Re}({}_\tau J_\mathbf{k} \tau_\mathbf{k}^*), \\ TT(\mathbf{k}) &= \mathrm{Re}({}_\psi J_\mathbf{k} \psi_\mathbf{k}^*), \end{aligned} \tag{26a}$$

and for the barotropic model

$$\begin{aligned} E(\mathbf{k}) &= k^2|\psi_\mathbf{k}|^2, \\ D(\mathbf{k}) &= \mathrm{Re}(D_k \psi_\mathbf{k}^*), \\ F(\mathbf{k}) &= \mathrm{Re}(F_k \psi_\mathbf{k}^*), \\ T(\mathbf{k}) &= \mathrm{Re}(J_k \psi_\mathbf{k}^*). \end{aligned} \tag{26b}$$

These are, respectively, the baroclinic energy, the barotropic energy, the potential enstrophy, the dissipation by friction of baroclinic energy, barotropic energy dissipation, forcing through the mean shear of baroclinic energy, barotropic forcing, baroclinic energy transfer and barotropic energy transfer and similarly for the total energy for the one-layer model. The transfer terms for the two-level model also include transfer *between* baroclinic and barotropic modes. For each of these the one-dimensional isotropic spectra may be defined by summing over all wavenumbers in a band of given absolute wavenumber, i.e.,

$$EC(k) = \sum_{k \le |\mathbf{l}| < |\mathbf{k}|+1} EC(\mathbf{l}),$$

and the zonal spectra by summing over all y wavenumbers

$$EC(k_x) = \sum_{k_y} EC(\mathbf{k}).$$

Because of symmetry, the eddy statistics for all wavenumber quadrants are identical. Hence they are summed and presented simply as functions of positive wavenumbers.

For a general discussion of the energy flow and the equilibrium spectra in baroclinic quasigeostrophic models see Rhines (1977), Salmon (1980) and Haidvogel and Held (1980). A few additional points of interest will be discussed here. The isotropic energy spectra are displayed in Fig. 1. The one-layer simulations (Fig. 1c) have a spectral slope very close to k^{-4}. This has been previously found by Basdevant *et al.* (1981) using a much higher order viscosity, and others. However, note that in the two-layer simulations the spectral slope is much shallower, closer to k^{-3}. These results are probably partially dependent on the friction, since the simulations here are fairly viscous; it would be interesting to see comparable one- and two-layer simulations with a much higher resolution and a less viscous model. Certainly in the two-level simulations surface drag is relatively strong. Since drag imposes a scale-independent time scale, a balance between drag and nonlinear transfer would yield a k^{-3} spectrum, since this has a scale-independent eddy turnover time.[1] The eddy turnover time is a useful measure of the intensity of the turbulence.

[1] I thank R. Sadourny for pointing this out.

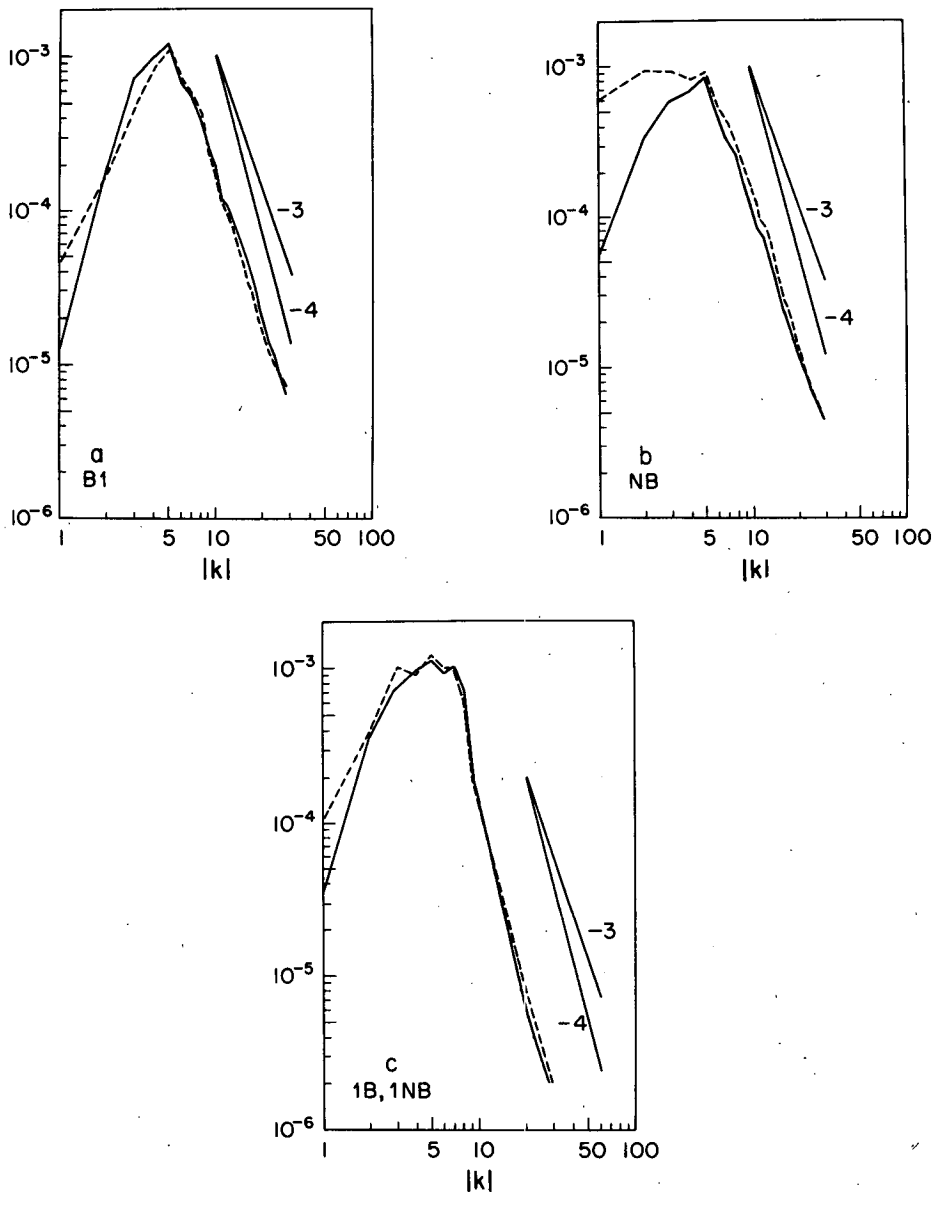

FIG. 1. Isotropic, barotropic and baroclinic energy spectra for (a) B1, (b) NB and (c) 1B and 1NB (total energy). In (a) and (b) the barotropic energy is a solid line, the baroclinic energy dashed. In (c), 1B is solid and 1NB dashed. The units are the arbitrary ones of the nondimensional numerical model.

It may be defined by (see McWilliams and Chow, 1981):

$$t_e = \left[\frac{k^{-3}}{E(k)}\right]^{1/2},$$

where k is the wavenumber and $E(k)$ an energy spectrum. The time t_e is a constant for a k^{-3} spectra. In these two-layer simulations eddy turnover times are of order 1 day (see Table 1) if the barotropic spectra alone are used. Note that the barotropic and baroclinic energies in B1 are very small at low wavenumbers, whereas the baroclinic energy and, to a lesser extent, the barotropic energy, is high when beta is zero. However, the zonal spectra (Fig. 2) are much more energetic at low k_x when beta is nonzero, especially in the barotropic modes.

An examination of the energy budgets is instructive (see Figs. 3 and 4). In B1, the case with a realistic beta, baroclinic instability of the mean shear (the only source of energy) provides a maximum input of energy at wavenumbers 5 and 6. These are not the wavenumbers of maximum linear instability which are

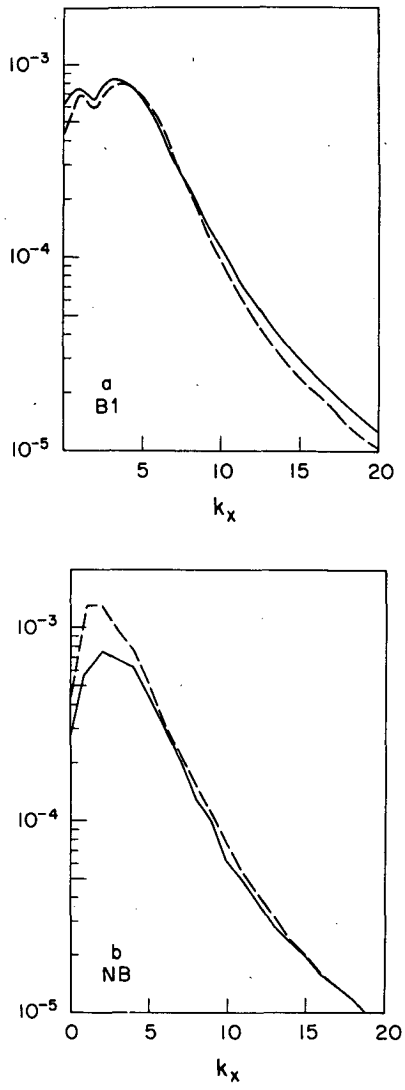

FIG. 2. Zonal energy spectra for (a) B1 and (b) NB. In both figures, the barotropic energy is a solid line, the baroclinic energy dashed.

slightly higher. Maximum energy input occurs where $\mathrm{Im}\{k_x\psi_{\mathbf{k}}\tau_{\mathbf{k}}^*\}$ is maximized, since $FC(\mathbf{k}) = (\lambda^2 - k^2)/k^2FT(\mathbf{k}) = \mathrm{Re}\{U(\lambda^2 - k^2)ik_x\psi_{\mathbf{k}}\tau_{\mathbf{k}}^*\}$. Transfer of energy occurs, not primarily to other baroclinic wavenumbers but to the barotropic modes, where it is further transferred to the gravest modes and dissipated. That energy is transferred from baroclinic to barotropic modes can be seen by noting that the areal integral of T in Fig. 3b is negative, and positive in Fig. 3a. In Fig. 3c the area under the T curve is zero. The small amount of baroclinic energy in the largest scales appears in fact to be due to friction which acts to *create* baroclinic energy. The formulation of surface drag used here is such that total energy must be dissipated. However, since it acts only on the lower

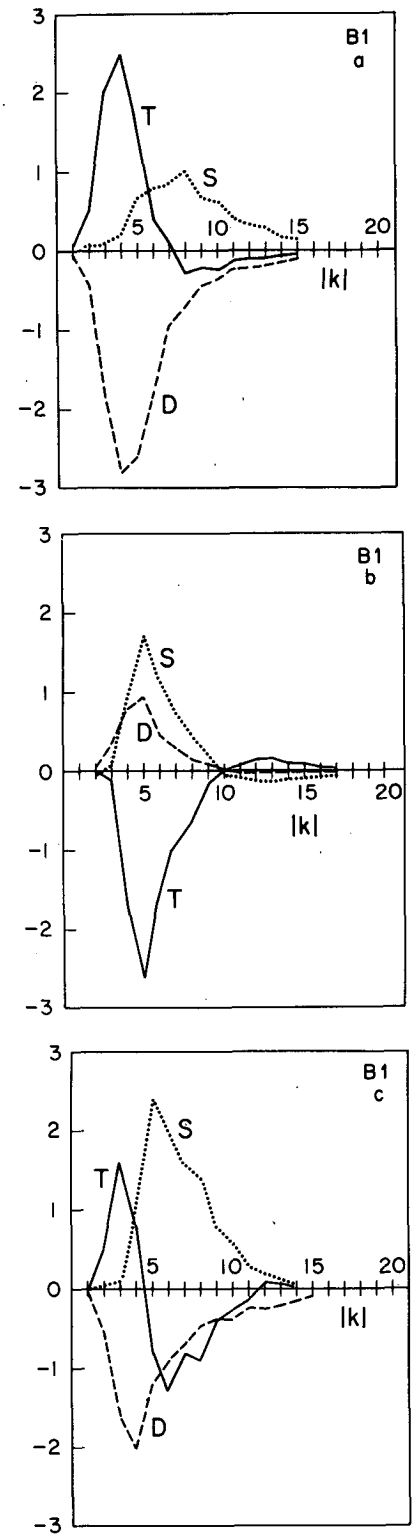

FIG. 3. Isotropic energy budgets for B1 where (a) is the barotropic budget, (b) the baroclinic budget and (c) the total. The labels S, D and T denote contributions by forcing (i.e., linear baroclinic instability), dissipation and transfer. (See text for a complete explanation.)

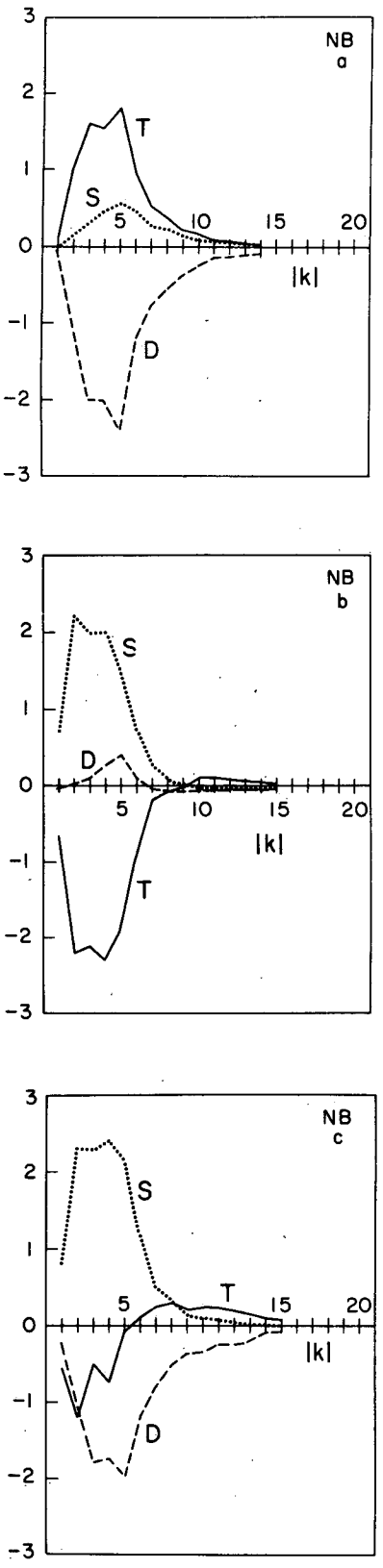

FIG. 4. As in Fig. 3, but for NB.

model layer, baroclinic energy, proportional to the square of the difference of the streamfunction between the two layers, may be increased. Romea (1977) also discusses the effect of surface drag in baroclinic instability. He shows that it can be a destabilizing influence on marginally stable modes. The total (baroclinic plus barotropic) energy budget shows an input of energy mainly between wavenumbers 5 and 10, a transfer to larger scales where it is destroyed by friction. In the case of zero beta (NB) baroclinic linear instability provides a baroclinic energy source in much lower wavenumbers (Green, 1960). Transfer occurs almost immediately and mainly to barotropic modes (plus a little to higher baroclinic wavenumbers) where friction provides a sink. The total energy budget displays a small transfer of energy toward *higher* wavenumbers arising from the transfer on the baroclinic modes. However, the total energy budget in NB is characterized by a *smaller* amount of transfer between scales than when beta is non-zero; it has a much more local nature.

The numerical simulations are consistent with the analytic arguments of Sections 3a and 3b in showing the movement of energy to the large scales, and the predilection for zonal motion when beta is realistic. However, they also show how the position of the energy injection scale is such as to increase the nonlinear energy transfer when beta is nonzero.

4. Predictability experiments

The general form of the predictability experiments is as follows. The model is integrated from random initial conditions until equilibrium is achieved. The integration is then continued for several weeks, to create the control integration. The "forecast" is obtained by perturbing the potential vorticity at the beginning of the control experiment and then stepping the model until these fields have completely diverged from those in the control experiment. The forcing and friction are maintained throughout all integrations. The usual form of the initial perturbation is a dephasing of the spectral coefficients of the potential vorticity such that the phase difference between the control and the perturbation increases from 0 to π as $|k|$ increases from 12 to 24, except for a multiplication by a random number selected uniformly on the interval $(-1, +1)$. Thus, the initial phase difference between control and forecast increases stochastically above wavenumber 12 until total decorrelation is achieved at wavenumber 24. The amplitude of the modes is unaltered. Most results are each from an ensemble of four experiments.

a. Error diagnostics

For each diagnostic defined in (26) we may define the corresponding error field by substituting the error

streamfunction ψ'_k or τ'_k and the error, or difference, forcing term. In particular, the error baroclinic and barotropic energies are

$$EC'(\mathbf{k}) = (k^2 + \lambda^2)|\tau'_{\mathbf{k}}|^2,$$

$$ET'(\mathbf{k}) = k^2|\psi'_{\mathbf{k}}|^2,$$

where $\psi' = \psi_1 - \psi_2$, where ψ_1 and ψ_2 are the streamfunctions of the two simulations, similarly for τ. The error energy ratio, or relative error, is defined by

$$EC'_r(k) = \frac{\sum_{|\mathbf{k}|\le|\mathbf{l}|\le|\mathbf{k}|+1} EC'(\mathbf{l})}{\sum_{|\mathbf{k}|\le|\mathbf{l}|\le|\mathbf{k}|+1} EC(\mathbf{l})},$$

and similarly for the barotropic fields.

b. *One-level integrations*

Fig. 5 illustrates the isotropic error energy ratio growth for the barotropic simulations. This figure (and Figs. 9, 10 and 11) illustrate the relative error, as a function of wavenumber, at various times marked in days after the initial perturbation ($t = 0$). The random number sequence in the forcing G_n [Eq. (8)] is the same for all runs. The conclusions reached from these simulations are consistent with the results of Holloway (1982) and Basdevant *et al.* (1981), and are presented only briefly here:

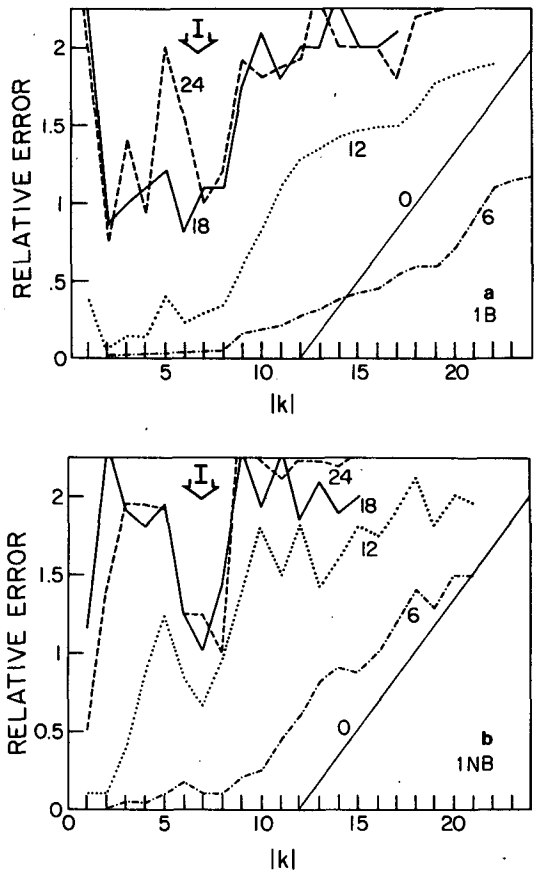

FIG. 5. Ratio of isotropic error energy to isotropic equilibrium energy at various times (marked in days) in one-layer integrations for (a) 1B and (b) 1NB. The abscissa is wavenumber. Beyond wavenumber 24, the error at time zero becomes parallel to the abscissa.

1) The effect of beta is to increase the overall predictability of the flow.

2) Predictability times are increased in the higher wavenumbers, perhaps more than in the lower wavenumbers in spite of beta scaling out of the equations at high wavenumbers.

3) The predictability time of the gravest mode $k = 1$, is *reduced* by beta, to the point where it is *less* predictable than the $k = 2, 3, 4$ modes. In Holloway's finite equivalent depth simulations, this phenomenon seems less apparent.

4) The predictability, not shown here, of the zonal flow ($k_x = 0$) *is* increased by beta, and is greater than the predictability of the $k_x = 1, 2, 3$ modes.

5) At the injection scale (I in Fig. 5) the decorrelation times are large. No error energy is injected here, and so error in these scales is swept away by the energy and enstrophy cascades. Eventually, though, these scales do become unpredictable.

5. Two-layer predictability

In considering the predictability of baroclinic flow, I shall be particularly concerned with the following questions:

(i) Does the restoring effect of beta carry through to the two-level case and still enhance predictability?

(ii) What are the effects of baroclinic instability on the flow decorrelation?

(iii) Does the odd behavior of the $k = 1$ mode arise in the two-layer experiments?

(iv) What effect does the form of the initial error have on the subsequent error growth?

Attention will be focused mainly on experiments B1 and NB.

a. *Physical space error*

A useful guide to the growth of error is gained by looking at the divergence of two fields in physical space. Fig. 6 illustrates the barotropic streamfunctions for two integrations and their difference, at a sequence of times separated by three days for a particular predictability experiment in the B1 ensemble. The contour interval for the difference field is the same as that of the synoptic field. The error field initially shows a structure richer in the smaller scales; as time progresses, the error field gains a larger scale component as the long waves become contaminated.

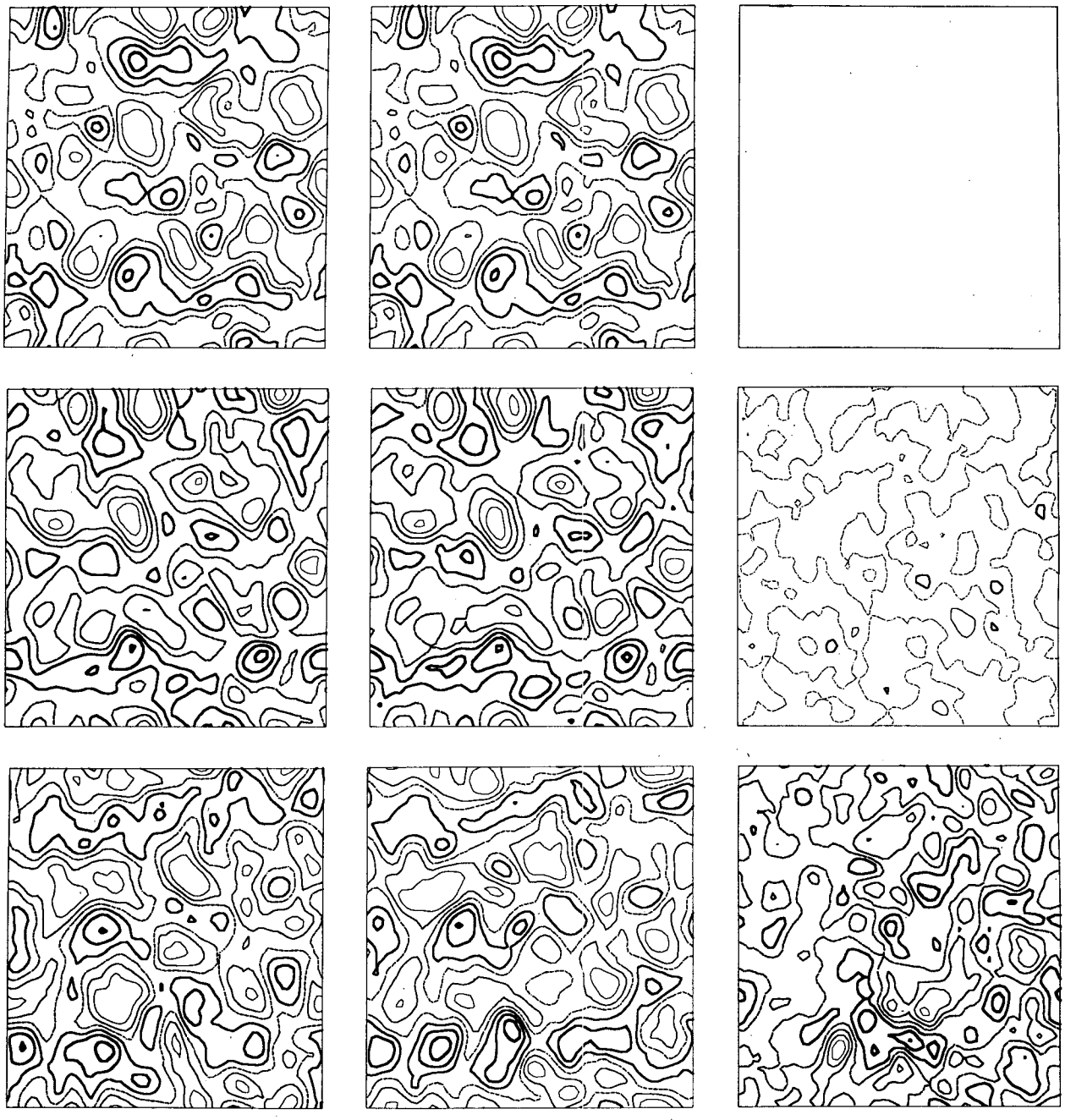

FIG. 6. A sequence of barotropic streamfunctions, in one predictability experiment in B1 at 3-day intervals. The two leftmost pictures are the two integrations, differing slightly at time zero. The rightmost picture is the difference streamfunction. Zero contour is dotted. Lighter contours have higher values. Contour interval is the same for the difference streamfunctions.

After nine days of integration, even when there is still some apparent skill left in the long-wave forecast (see Fig. 9), the two fields bear little resemblance to each other.

The error streamfunction fills the domain fairly uniformly, i.e., it does not display any patchiness. The largest errors arise where one or the other original streamfunctions is an extrema.

b. Total error

It is somewhat difficult to isolate the effects of wave propagation in a two-layer model because the linear stability properties are greatly affected by beta. Experiments B1 and NB have the same supercritical shear and approximately the same time-averaged total energy and therefore seem comparable. If the same

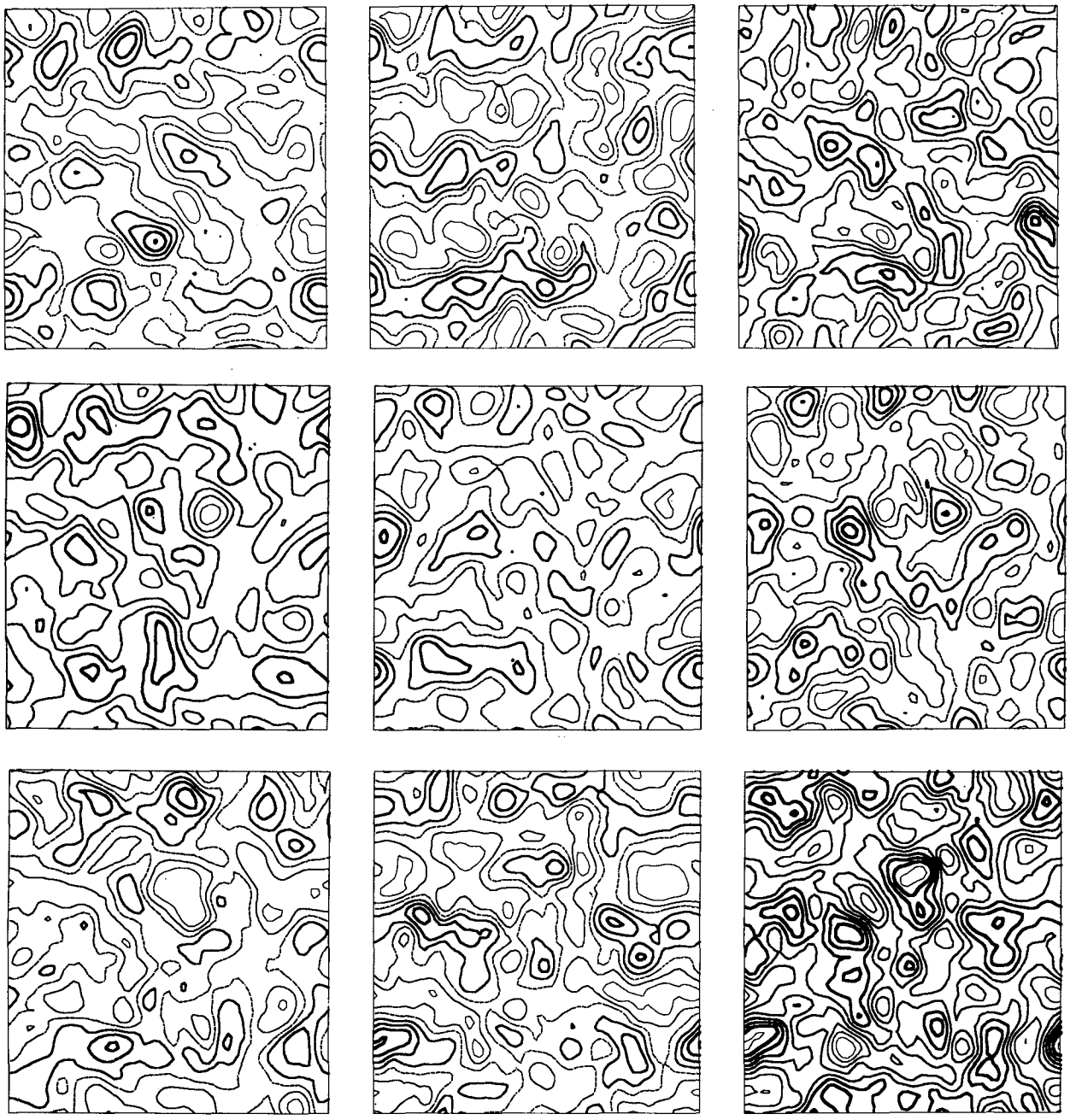

FIG. 6. (*Continued*)

absolute shear had been used for the two cases, the experiment with zero beta would have been much more supercritical and would have had much more intense turbulence. Another reasonable choice would have been to compare runs with the same eddy turnover time. Since B1 has less energy in the low wavenumbers it has more energy in high wavenumbers and a smaller eddy turnover time than NB. An increased eddy turnover time would have increased the predictability of B1 slightly, although it would still be very similar to that of NB. Examination of Fig. 7 reveals that the total predictability of the flow is *not* enhanced by the beta effect, nor is there any significant difference between barotropic and baroclinic modes.

Consider the error energy budget. This may be

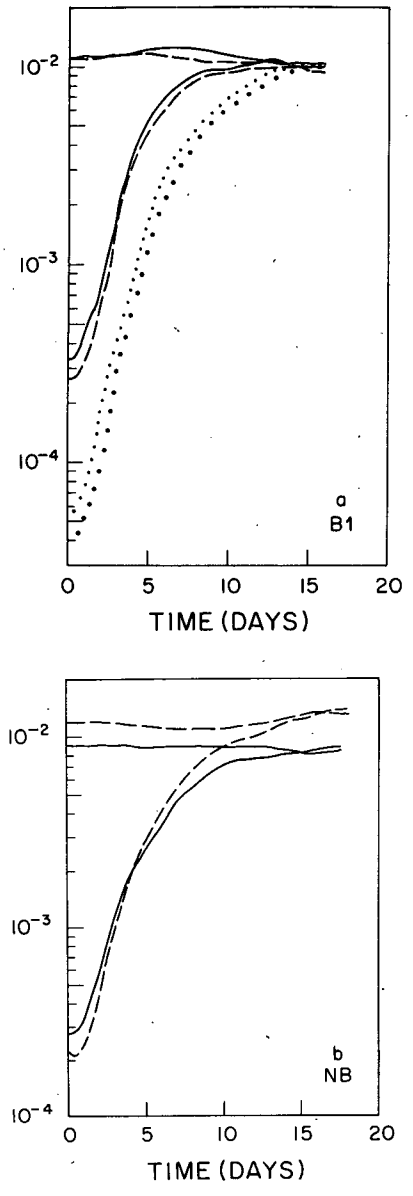

FIG. 7. Total error energy growth for (a) B1 and (b) NB. The barotropic energy is a solid line, the baroclinic is dashed. The dotted curves in (a) are the barotropic error growths for initial errors confined to $k > 24$, and $k > 28$. Otherwise, initial error is confined to $k > 12$. The almost horizontal curves show twice the control energy for one integration from the ensemble, illustrating a typical time variation of total energy.

written (where a prime denotes the difference, or error field):

$$\frac{d}{dt}\{k^2|\psi'_{\mathbf{k}}|^2 + (k^2+\lambda^2)|\tau'_{\mathbf{k}}|^2\}$$

$$= \mathrm{Re}({}_{\tau}F'_{\mathbf{k}}\tau'^{*}_{\mathbf{k}} + {}_{\psi}F'_{\mathbf{k}}\psi'^{*}_{\mathbf{k}}\} + \mathrm{Re}\{{}_{\tau}D'_{\mathbf{k}}\tau'^{*}_{\mathbf{k}} + {}_{\psi}D'_{\mathbf{k}}\psi'^{*}_{\mathbf{k}}\}$$

$$+ \mathrm{Re}\{{}_{\tau}J'_{\mathbf{k}}\tau'^{*}_{\mathbf{k}} + {}_{\psi}J'_{\mathbf{k}}\psi'^{*}_{\mathbf{k}}\}. \quad (27)$$

The terms on the right-hand side (rhs) represent the effects of forcing by the mean shear, dissipation and transfer on the error energy, respectively. When summed over all wavenumbers, the last term on the rhs of (27) does *not* vanish: the Jacobian terms are able to *create* error energy, as well as distribute it across wavenumbers. Fig. 8 shows the error creation by linear baroclinic instability and by nonlinear interactions. The total error creation by nonlinear effects is much the same when beta is zero, but the

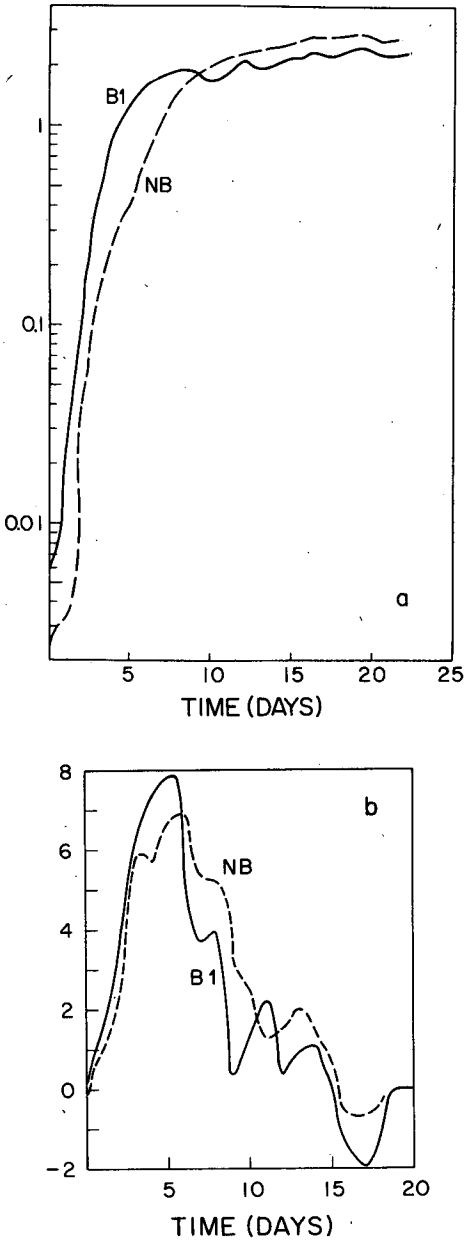

FIG. 8. Error energy creation in B1 and NB due to (a) baroclinic instability of the mean flow and (b) nonlinear transfer. Units are comparable.

linear creation is significantly smaller for the first ten days. Recall that the effect of beta is to increase the wavenumber at which baroclinic instability is greatest, and that the energy input is proportional to the magnitude of the streamfunction. For zero beta, instability occurs at very low wavenumbers. For a long time the error in these modes is very small and linear baroclinic instability is an inefficient mechanism for creating error.

Even though weakly nonlinear theory suggests energy transfer should be slowed by beta in the baroclinic case, just as in the one-layer case, error creation by wave-wave interaction is no smaller when beta is non-zero. Note that, for zero beta, energy transfer is confined largely to low, well predicted wavenumbers. There is now *less* communication between the low wavenumbers and the contaminated smaller scales, and any energy flow is toward higher wavenumbers. For the zero beta case (NB) error propagation, then, is generally against energy transfer, whereas in the realistic beta case error propagation is with energy transfer. Thus for the two-layer case there is no longer any *a priori* reason why error propagation and creation will be larger when beta is zero.

The predictability times of the two-layer model are significantly shorter than those of the one-layer integrations, in spite of the barotropic energy of the two-layer models being about the same as the energy in the one-layer integrations. In the barotropic vorticity Eq. (7) the terms $J(\tau, \nabla^2\tau)$ and $U\partial(\nabla^2\tau)/\partial x$ appearing in (9) are parameterized by a forcing uncorrelated with the flow. In the two-layer simulations these provide an additional source of error, reducing the decorrelation time. In the two-layer case, balance in the error energy budget is ultimately achieved through the balance of the linear source term with the dissipation: the Jacobian terms (on average, but not necessarily instantaneously) can therefore provide no net contribution. In the one-layer case, however, where the energy source term provides no error, the dissipation is balanced by the nonlinear terms which grow more or less monotonically before levelling off at a positive value.

The predictability time is seen to be lengthened by

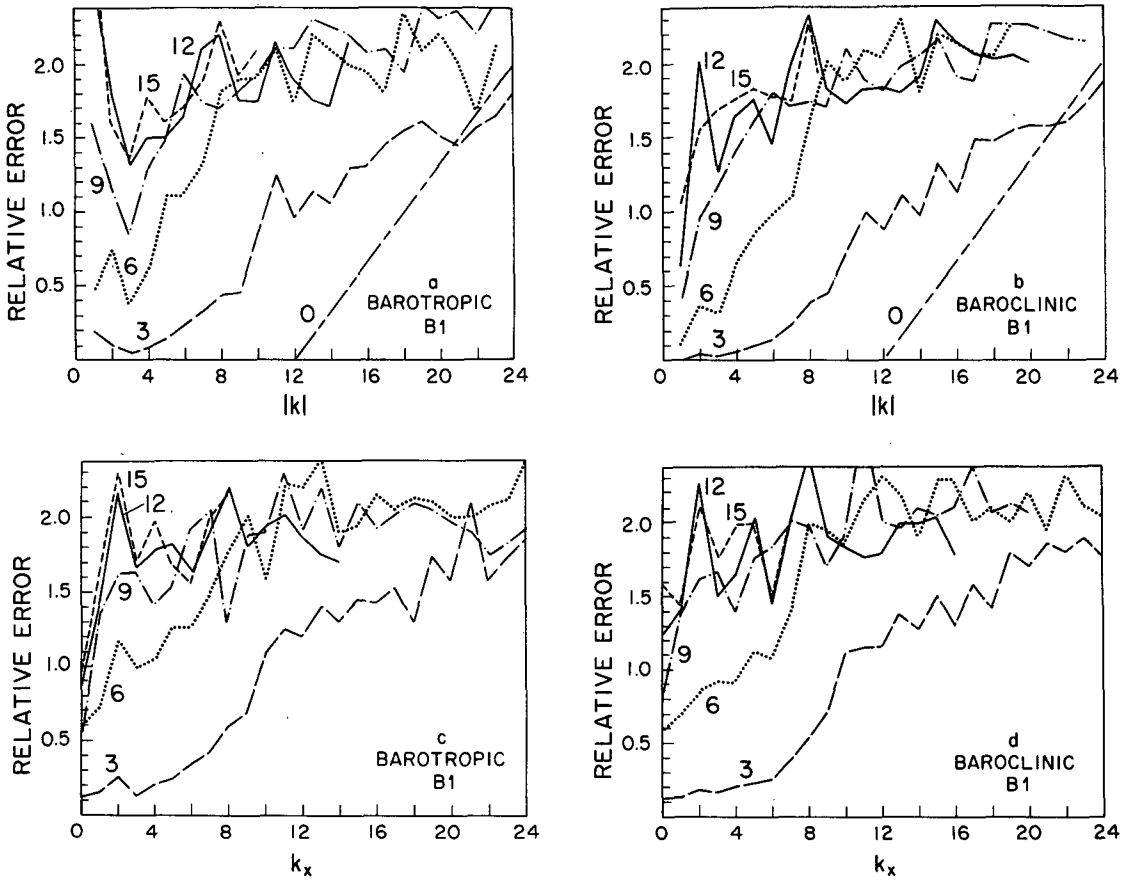

FIG. 9. Relative error growth for B1: (a) isotropic barotropic error, (b) isotropic baroclinic error, (c) zonal barotropic error and (d) zonal baroclinic error.

reducing the initial error. The lower dotted curves in Fig. 7a are obtained with initial errors only above wavenumber 24 and above wavenumber 28, respectively. The initial error doubling rate is slightly larger when the error is confined to smaller scales—the average error doubling time in the case of the smallest initial error is 0.85 days (during the first five days of the experiment) whereas it is 1.0 days in the standard experiment. To ascertain whether still smaller scale initial errors could produce still larger initial error doubling times, and always yield finite predictability times as Lorenz (1969) suggested, requires a much higher resolution model than this one. A reduced mean baroclinicity also enhances the predictability times: when the mean shear was reduced from 7.5 m s^{-1} (in B1) to 4. m s^{-1} (in B2) the predictability times rose by approximately a factor of 2.

c. *Error spectrum*

The error ratio spectra are given in Figs. 9 and 10. The figures show both the isotropic and zonal spectra of relative errors for various times (marked in days) for B1 and NB, with the "standard" initial perturbation. The dominant feature is that of error spreading into and growing in the smaller wavenumbers. No artificial predictability at the energy injection scale is present. Predictability in the small scales (above wavenumber 10) is lost completely after approximately 6 days in B1, and shortly thereafter in NB. Predictability in the long waves persist much longer. Indeed the forecast of the long waves (k = 2, 3, 4) generally shows skill up to ~15 days. The skill time generally increases monotonically as wavenumber decreases, for two reasons. First, error is spreading in from longer wavenumbers and unless energy transfer is completely non-local in spectral space the larger scales will be contaminated last. Second, the turbulent interaction rate may be expected to increase as the scale is reduced (cf. Lorenz, 1969); thus information will be lost in the high wavenumbers first. If beta is non-zero, interactions among low wavenumbers are further inhibited, and the effect will be more noticeable. Fig. 11 shows the barotropic error spectra for an experiment in which all wavenumbers were dephased equally (with a random modifier). Even though the initial error ratio is the same for all wavenumbers, the forecast skill, or predictability, is lost

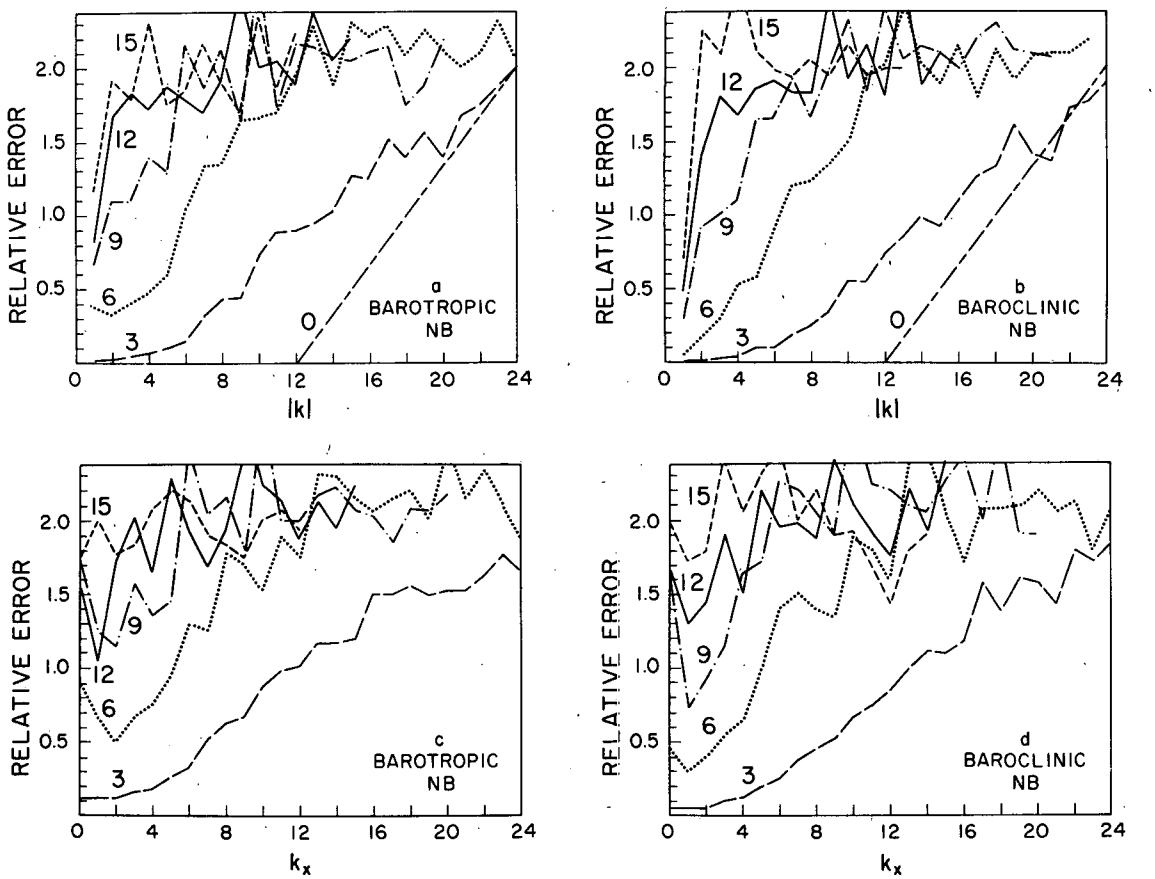

FIG. 10. As in Fig. 9, but for NB.

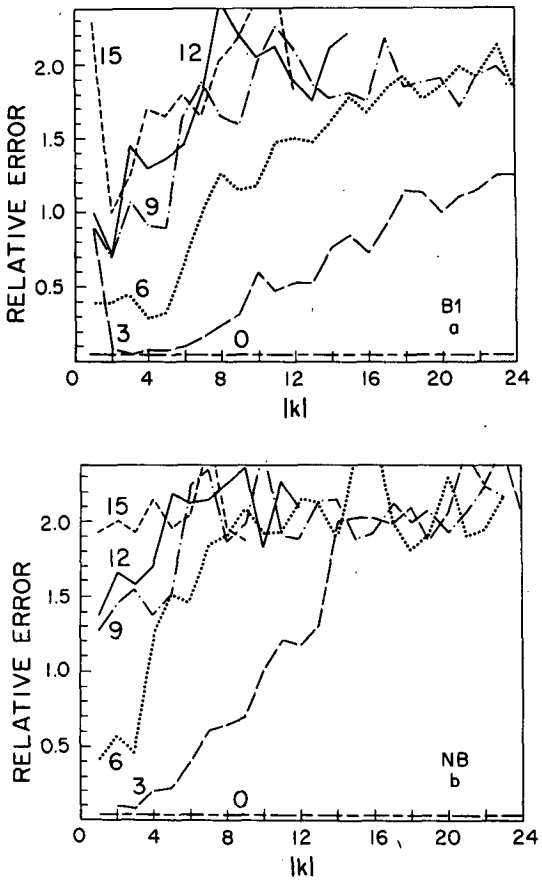

FIG. 11. Relative isotropic barotropic error growth for (a) B1 and (b) NB, in which initial relative error is white.

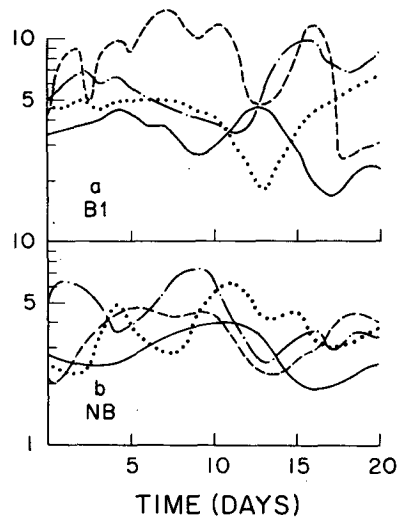

FIG. 12. Amplitude of various $k = 1$ and $k_x = 0$ modes with time for one realization in (a) B1 and (b) NB. Dashed line is $k = 1$, barotropic; solid line is $k = 1$, baroclinic; dot-dashed line is $k_x = 0$, barotropic; and dotted line is $k_x = 0$, baroclinic.

first in the higher wavenumbers. Thus the long waves are *intrinsically* more predictable than short waves.

A noticeable feature of the error when beta is realistic is that the $k = 1$ barotropic mode is markedly less predictable than the $k = 2, 3, 4$ modes. The effect does not arise in the baroclinic modes, or when the spectra are decomposed into a zonal spectra, or when beta is zero. It arises because the barotropic $k = 1$ mode is extremely unenergetic when beta is non-zero. Interactions with more energetic spectral neighbors can therefore cause it to gain or lose a relatively large portion of its energy in a relatively short amount of time, as Fig. 12 illustrates. This shows a typical time sequence of various $k = 1$ and $k_x = 0$ modes for B1 and NB. It is clear that the amplitude of the barotropic $k = 1$ mode in B1 may fluctuate by as much as a factor of 4 in the course of less than a day, a much more rapid fluctuation than is ever the case when $\beta = 0$.

d. The results of McWilliams and Chow

Recently, McWilliams and Chow (1981; MC henceforth) found no evidence for enhanced predictability due to wave propagation in a baroclinic channel model. The mechanisms identified above certainly appear to be consistent with their results, and to be at least a partial explanation. However, MC's model does differ somewhat from that used here (forced, wind-driven channel model versus a periodic, homogeneous model with essentially a fixed mean baroclinic structure). Also, their relative error appears to be fairly uniform with wavenumber, whereas here it tends to increase with wavenumber, both with and without beta. Clearly, the fair test would be to use MC's model with a variety of beta values, although there seems to be no reason why the effects described in this paper should not be applicable in more complex situations, such as MC's.

6. Summary and conclusions

This study has been concerned with the equilibrium fields and predictability properties of two-layer flow on a beta-plane. The work may be considered an extension of the work of Lilly (1972), Basdevant *et al.* (1981) and Holloway (1982) to include the effects of vertical stratification and baroclinicity.

Beta has somewhat richer effects in two-layer flow than in barotropic flow. The baroclinic instability of the long waves is inhibited by a mean gradient of potential vorticity, and energy enters the system at a higher wavenumber. When beta is zero, energy enters primarily in baroclinic modes at low wavenumbers and attempts to pass to still lower wavenumbers. This can only be achieved by a conversion to barotropic energy, with a smaller amount of energy being transferred to higher baroclinic wavenumbers, an in-

efficient process. This contrasts with the case when beta is non-zero, where energy cascades to smaller wavenumbers. Weakly nonlinear theory for the case of non-zero beta suggests that energy will tend to move away from higher frequencies, and toward low wavenumbers. Thus zonal barotropic modes are the preferred end-state in two-layer flow, as in one-layer flow. The low wavenumbers are energetically very weak when beta is non-zero.

The predictability properties of two-layer flow are likewise rather subtly affected by beta. In contrast to the case with one-layer flow, the presence of beta does not automatically and significantly increase the decorrelation time in two-layer flow, even though we may still expect energy cascades in low wavenumbers to be slowed by beta. In one-layer simulations, energy is generally artificially injected around wavenumber 8 whether beta is zero or not. The energy cascade to low wavenumbers is accompanied by an enstrophy cascade to high wavenumbers. Beta slows the energy cascade, and hence the enstrophy cascade (Rhines, 1975), and so increases predictability in all wavenumbers. In two-layer flow energy enters at very small well-predicted wavenumbers when beta is zero; hence error is injected much less efficiently than when beta is non-zero. Second, and more importantly, when beta is zero, energy is entering the system at low wavenumbers and cannot be transferred to still lower wavenumbers. Thus, the nonlinear energy transfer is concentrated in the relatively well predicted low wavenumbers, again meaning error is created (by nonlinear transfer) at least as efficiently when beta is non-zero. For now not only is there more energy transfer but it is in the same direction as error propagation.

The predictability of the gravest barotropic mode ($k = 1$) is lessened by beta, although the effect is not important in this model since this mode has little energy. This mode varies erratically in amplitude and phase because of its extreme weakness, and so tends to be unpredictable.

The predictability of the zonal flow *is* increased by beta, because of the production of strong, steady zonal currents.

Reducing the mean baroclinicity reduces the energy levels in the model and increases the predictability time.

The error energy ratio is generally less in lower wavenumbers, even when the initial error is distributed evenly across wavenumbers. This is the case even when beta is zero, and is due to the longer turnover, or eddy interaction time for the long waves. It is patently the case that the initial (observational) relative error in weather forecasts is larger in the smaller scales. However, the above result implies that even with no direct forcing the long waves are intrinsically more predictable than the short waves, a result independent of the initial error conditions.

The work raises a number of possible avenues of future research. Two-layer models with homogeneous forcing plainly fail to reproduce the intensity of the low-wavenumber energy spectra observed in the real atmosphere. Two likely causes for this are inadequate vertical resolution (J. Roads, personal communication, 1982) and the lack of topography, and it would be interesting to perform experiments to see to what extent either is responsible. We may also expect the effects of topography on predictability to be considerable. For example a low-wavenumber stationary forcing (e.g., by orography, or land-sea temperature contrasts) may enhance the predictability of the long waves, yet the synoptic-scale predictability may be unaltered. In general it would be interesting to study the importance of the spectral location of the energy source and hence the direction of the ensuing energy transfer relative to the direction of the error transfer, perhaps using a barotropic model where the energy source can be controlled. These and other investigations using simplified models will be important in evaluating the effects of the variety of influences on predictability.

Acknowledgments. I would like to thank J. O. Roads and R. C. J. Somerville for their continual help and advice, and G. Holloway, A. A. White and the referees for their comments on the manuscript. My thanks also go to R. L. Salmon who kindly provided a code for the Jacobian calculations, and to G. A. Johnston for her skillful typesetting. The work was funded by the California Space Institute under Grant CS-78-81 and the National Science Foundation under Grant NS7 ATM82-10160.

REFERENCES

Asselin, 1972: Frequency filter for time integrations. *Mon. Wea. Rev.*, **100**, 487–490.

Basdevant, C., B. Legras, R. Sadourny and M. Beland, 1981: A study of barotropic model flows: Intermittency, waves and predictability. *J. Atmos. Sci.*, **38**, 2305–2326.

Bender, C., and S. A. Orszag, 1978: *Advanced Mathematical Methods for Scientists and Engineers.* McGraw-Hill, 593 pp.

Charney, J. G., R. G. Fleagle, V. G. Lally, H. Riehl and D. G. Wark, 1966: The feasibility of a global observation and analysis experiment. *Bull. Amer. Meteor. Soc.*, **47**, 200–220.

Fjørtøft, R., 1953: On the changes in the spectral distribution of kinetic energy for two dimensional, nondivergent flow. *Tellus*, **5**, 225–230.

Green, J. S. A., 1960: A problem in baroclinic stability. *Quart. J. Roy. Meteor. Soc.*, **86**, 237–251.

Haidvogel, D. B., and I. M. Held, 1980: Homogeneous quasi-geostrophic turbulence driven by a uniform temperature gradient. *J. Atmos. Sci.*, **33**, 2044–2660.

Hasselmann, K., 1967: A criterion for nonlinear wave stability. *J. Fluid. Mech.*, **30**, 737–739.

Holloway, G., 1979: On the spectral evolution of strongly interacting waves. *Geophys. Astrophys. Fluid Dyn.*, **11**, 271–287.

——, 1983: Effects of planetary wave propagation and finite depth on the predictability of atmospheres. *J. Atmos. Sci.*, **40** (in press).

Jones, S., 1979: Rossby wave interactions and instabilities in a

rotating, two layer fluid on a beta-plane. Part I: Resonant interactions. *Geophys. Astrophys. Fluid Dyn.*, **11**, 289–322.

Kenyon, K., 1964: Nonlinear energy transfer in a Rossby-wave spectrum. Geophysics Fluid Dynamics Program, Woods Hole, MA, 69–83.

Leith, C. E., 1971: Atmospheric predictability and two-dimensional turbulence. *J. Atmos. Sci.*, **28**, 145–161.

——, and R. H. Kraichnan, 1972: Predictability of turbulent flows. *J. Atmos. Sci.*, **29**, 1041–1058.

Lilly, D. K., 1972: Numerical simulation studies of two-dimensional turbulence: II Stability and predictability studies. *Geophys. Fluid Dyn.*, **4**, 1–28.

Lorenz, E. N., 1963: The mechanics of vacillation. *J. Atmos. Sci.*, **22**, 448–464.

——, 1969: The predictability of a flow which possesses many scales of motion. *Tellus*, **21**, 289–307.

McWilliams, J. C., and J. Chow, 1981: Equilibrium geostrophic turbulence, I: A reference solution in a beta-plane channel. *J. Phys. Oceanogr.*, **11**, 921–949.

Orszag, S. A., 1971: Numerical simulation of incompressible flow within simple boundaries. *Stud. Appl. Math.*, **L**, 293–327.

Rhines, P. B., 1975: Waves and turbulence on a beta-plane. *J. Fluid Mech.*, **69**, 417–443.

——, 1977: The dynamics of unsteady currents. *The Sea*, Vol. 6, E. A. Goldberg, I. N. McCane, J. J. O'Brien and J. H. Steele, Eds., Wiley, 189–318.

Romea, R. D., 1977: The effects of friction and beta on finite amplitude baroclinic waves. *J. Atmos. Sci.*, **34**, 1689–1695.

Salmon, R. L., 1978: Two-layer quasi-geostrophic turbulence in a simple special case. *Geophys. Astrophys. Fluid Dyn.*, **10**, 25–52.

——, 1980: Baroclinic instability and geostrophic turbulence. *Geophys. Astrophys. Fluid Dyn.*, **15**, 167–211.

Thompson, P. D., 1957: Uncertainty of initial state as a factor in the predictability of large scale atmospheric flow patterns. *Tellus*, **9**, 275–295.

Williams, G. P., 1978: Planetary circulations: I. Barotropic representation of Jovian and terrestrial turbulence. *J. Atmos. Sci.*, **35**, 1399–1426.